Anisotropy of the Threshold Energy for Production of Frenkel Pairs in Copper and Platinum

P. Jung, R. L. Chaplin,* H. J. Fenzl, K. Reichelt, and P. Wombacher
Institut für Festkörperforschung, Kernforschungsanlage Jülich, Germany
(Received 13 December 1972)

Thin copper and platinum single-crystal foils have been irradiated at liquid-helium temperature with electrons of energies between 1 and 3 MeV. From resistivity measurements the directional dependence of the damage rate was determined with high accuracy by varying the orientation of the foils relative to the direction of the beam of the irradiation electrons. From the dependence of defect production on electron energy and foil orientation, the angular dependence of the threshold displacement energy could be determined. In both fcc metals, the closest-packed directions ⟨110⟩ and ⟨100⟩ possess ring-shaped regions which show minimum threshold values down to 19 eV for copper and 33 eV for platinum, while maximum threshold values are attained near the ⟨111⟩ direction. For the electrical resistivity per unit concentration of Frenkel pairs, we obtained $(1.7 \pm 0.3) \times 10^{-4}$ $\mu\Omega$ cm for copper and $(9.5 \pm 0.5) \times 10^{-4}$ $\mu\Omega$ cm for platinum. For copper a comparison with other theoretical and experimental works is possible and shows satisfactory accordance.

I. INTRODUCTION

The threshold energy is an important quantity for describing the behavior of a solid under irradiation. It equals the minimum recoil energy a lattice atom must receive from an irradiating particle to be permanently displaced from its lattice site. Owing to the atomic structure of a lattice, the threshold energy should be anisotropic. Knowledge of this directional dependence of the threshold energy may lead to some conclusions on defect production mechanisms and possibly on the configurations of stable Frenkel pairs.

There are two principal ways to determine the directional dependence of threshold energy. One is a theoretical attempt to simulate damage processes in solids in a computer starting from some assumed interatomic potential. The most comprehensive work on this procedure has been done at Brookhaven, giving threshold energy profiles for the fcc metal copper[1] and bcc iron.[2] The other technique is to assume a threshold energy profile, to calculate defect production rates from this profile, and to compare these values with experimental damage-rate data. This was done extensively in the case of silicon[3] and bcc tantalum.[4] Both methods have disadvantages: The theoretical method lacks precision, because up to now, no well-founded interatomic potential for the atomic forces is available, while the experimental method has its uncertainties in the measuring accuracy of the damage rate and a rather complicated propagation of this error to the resulting threshold energy profile. Despite this, as has been shown in the work on tantalum,[4] it is possible to derive a threshold energy profile from careful damage measurements.

Damage-rate measurements in copper single crystals have already been done, in the earlier work of Sosin and Garr[5] and Kamada *et al.*,[6] with electron energies up to 1 MeV. In both works the measuring accuracy was insufficient to get unambiguously the relative size of the damage rate in single crystals of different orientations. The main reason for this was the difficulty in comparing absolute damage rates in samples of different orientations. To avoid this uncertainty, we have measured damage rates in copper for electrons incident along different crystallographic directions by rotating the samples. On the other hand, our accelerator only provides electrons of energies above 1 MeV, which is markedly above the threshold of copper. Therefore we also did measurements on the heavier fcc metal platinum, where our electron energies of 1–3 MeV covered the whole region of low-energy damage.

II. EXPERIMENTAL DETAILS

The copper single-crystal foils had a thickness of 15 μm. They were obtained from bulk material by an electrolytic jet polishing method described in Ref. 7. After cutting and mounting the samples on the sample holder, they showed room-temperature-to-helium-temperature resistivity ratios RR between 300 and 1000. The remaining resistivity may be due to residual impurities or strain from cutting.

The single-crystal platinum foils were prepared by two different techniques. ⟨100⟩ and ⟨110⟩ samples have been obtained by epitaxial growth on pieces of rock salt covered with a thin layer of epitaxial silver. The platinum depositions had a thickness of 10 μm and RR values from 50 to 100. As epitaxial growth gives twins in the case of ⟨111⟩ crystals, the ⟨111⟩ orientations have been prepared by a strain-anneal technique starting from cold-rolled polycrystalline 10-μm foils and even-

tually giving grains with diameters up to 5 mm. The resistivity ratios of these samples, corrected for size effect, were up to 12 000, owing to the very pure starting material (99.999% pure).

The copper and the ⟨111⟩ platinum samples were cut by spark erosion to strips of about 15×1 mm, and thin wires were spot welded as potential leads. The shape of the platinum samples prepared by epitaxial growth was determined by a mask, which already included two appendages for resistivity measurement. Finally, the samples were spot welded pairwise on sample holders of aluminum oxide which, as already described,[4] could be rotated with respect to the irradiation beam. As foils of the same orientation normal to their surface were prepared with different orientations to their length axis, a certain lattice direction could be obtained in samples of different orientation depending on their rotation axis. Figure 1 shows how, by rotating a ⟨111⟩ foil around a ⟨110⟩ axis to 55°, the ⟨100⟩ direction becomes the irradiation direction, while the right-hand side of Fig. 1 shows that the ⟨100⟩ direction is also attainable by rotating a ⟨110⟩ foil around a ⟨100⟩ direction by 45°. Similarly, the ⟨110⟩ or the ⟨111⟩ direction and also the directions between the close-packed directions are attainable by rotating foils of different orientations.

Details of the cryostat and the irradiation technique have already been described.[4] However, we have used an improved system for measuring the beam current, which differs from the device reported there. It consisted of a beam shutter in front of the sample chamber with a tube and a cage for catching backscattered and secondary-emitted electrons. The electron flux monitored by this system was checked by measuring damage rates in polycrystalline aluminum, and the results gave good agreement with the data of Wurm *et al.*[8]

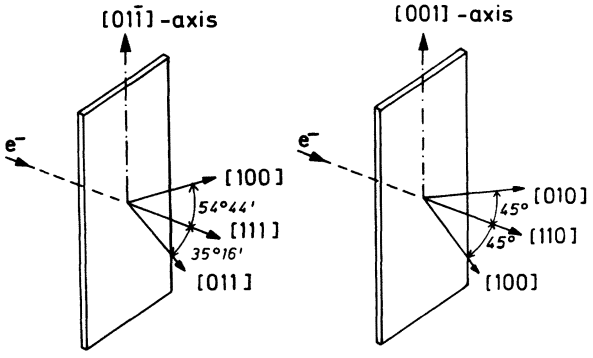

FIG. 1. Schematic view of changing the irradiation direction in single-crystal foils by rotation around different axis.

III. EXPERIMENTAL RESULTS

We have determined the relative damage rates for irradiation along different lattice directions by measuring the resistivity increase after irradiating samples in a certain rotated position and comparing it to a foregoing and a following damage-rate measurement in the zero position. From this, we got relative damage rates for all directions along the border of the fundamental triangle, that is, directions between the three main crystallographic directions in the cubic lattice, ⟨110⟩, ⟨100⟩, and ⟨111⟩.

For the evaluation of our data in terms of an anisotropic threshold energy it was sufficient to use only damage-rate data along the border of the fundamental triangle. As we know from our respective measurements on tantalum, these data always give a good representation of the variation of damage rate over the whole fundamental triangle. Results are shown in Figs. 2 and 3 for copper and platinum, respectively. The data are normalized to the value for the ⟨110⟩ direction. The energies written by each curve correspond to the average energy of the electrons in the foils, which lies about 0.05 MeV below the irradiation energy because of energy loss in the window and in the samples. Every datum point was obtained by averaging the results of at least two different samples, rotated to the same crystallographic position. Deviations from sample to sample amounted to about 4%, depending on direction and energy. Such errors may be caused by small differences in sample thickness and by slight misorientations of the single crystals on the sample holder.

While the relative damage rates of Figs. 2 and 3 showed no dependence on purity in different samples, the initial absolute damage rate seemed to be slightly increased in samples of lower resistivity ratio. Therefore, absolute damage rates were selectively derived from the purest foils which, for example, in the case of platinum, were the ⟨111⟩ samples. Values for the other directions are then obtained via the data in Figs. 2 and 3. The resulting values of the absolute damage rates for the three main crystallographic directions as a function of the maximum recoil energy T_{max} are shown in Figs. 4 and 5 for copper and platinum, respectively.

For both materials polycrystalline data also are included. The polycrystalline-copper data are from Wurm,[9] while the corresponding data for platinum (Fig. 5) are from our own measurements which, apart from the 3-MeV value, are in very good accordance with earlier measurements of Bauer and Göppinger[10] and Burke *et al.*[11] For both materials the polycrystals have damage-rate values lying between the single-crystal data, as

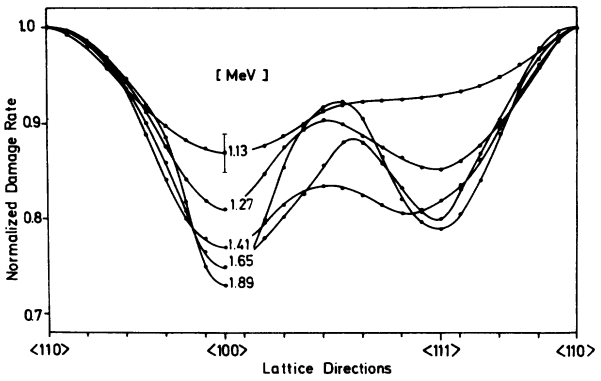

FIG. 2. Dependence of damage rate in copper on lattice direction and electron energy. The damage rates are normalized to the ⟨110⟩ value.

should be expected. For copper (Fig. 4) the measurements of Sosin and Garr[5] at energies below 1 MeV are included. The smooth connection of Sosin's values and our data at 1 MeV is an indication of the reliability of both data sets.

In the final part of this section some remarks are made about the corrections involved in the results of Figs. 2–5. To avoid the uncertainty of electrical size-effect corrections (compare Ref. 12) in the determination of our absolute damage rates, we used damage rates which have been obtained by extrapolating the linear part of the damage-rate–vs–resistivity curve of copper and platinum[12] to $\Delta\rho = 0$. Resulting values must then be

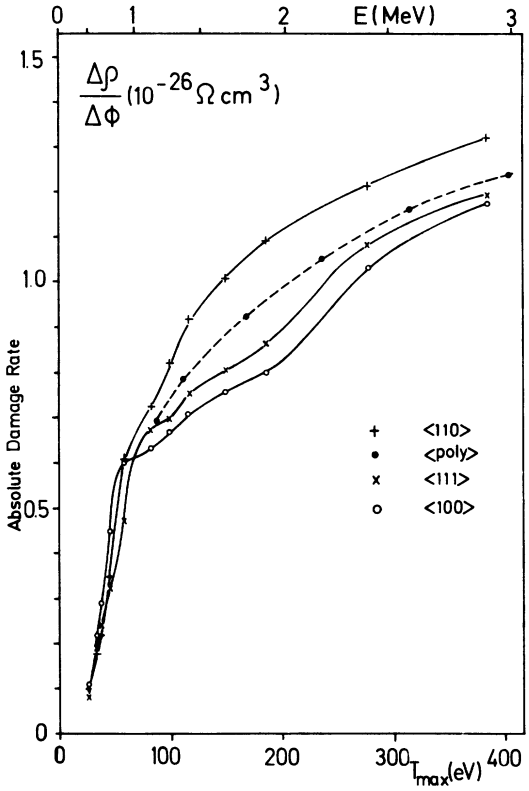

FIG. 4. Absolute damage rates of copper single crystal for irradiation along the three main crystallographic directions versus maximum recoil energy. The data below 1 MeV are from the work of Sosin *et al.* (Ref. 5). The polycrystalline data included are from Wurm (Ref. 9).

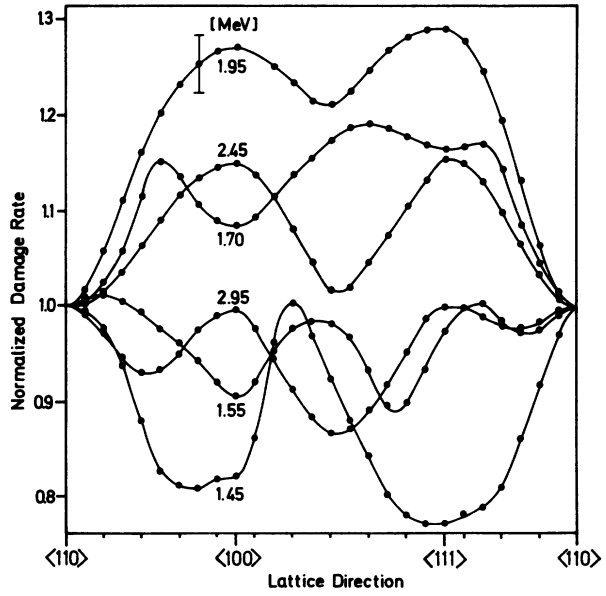

FIG. 3. Dependence of damage rate in platinum on lattice direction and electron energy. The damage rates are normalized to the ⟨110⟩ value.

corrected only for the increase of path length of the irradiation electrons due to multiple scattering in the samples. These corrections are described by a theory of Yang[13] and decrease from about 5 to 1.5% for platinum, and from 2 to 0.5% for copper, as electron energies increase from 1.5 to 3.0 MeV.

This effect of multiple scattering on effective path length also involves corrections to the normalized damage-rate data which arise from rotating the foils. Indeed, the increase in the effective thickness of a foil when electrons are obliquely incident is exactly compensated by a decrease of the flux of the irradiating particles. But to second order this increase in thickness by rotating the samples causes an increase of multiple scattering of the electrons. This results in a further increase in path length and, therefore, especially at low energies, in a slight increase in damage rate, which is shown in the upper curve of Fig. 6.

But instead of this small increase in damage rate caused by rotating the foils, a much larger decrease is observed at low energies, which is shown by the solid line in Fig. 6. This curve has

been obtained by comparing damage rates at 0° and 45° rotation angles in polycrystalline platinum and in single crystals; for example, by comparing the relative damage rates of a ⟨110⟩ sample being rotated by 45° to a ⟨100⟩ position, and conversely of a ⟨100⟩ sample rotated also by 45° to a ⟨110⟩ position. The observed strong decrease of the damage rates with rotation angle at energies close to threshold most probably results from the decrease of energy of the electrons when passing through the foils.

The average change of electron energy in 10 μm of platinum is about 0.02 MeV. At energies such that the damage rate changes appreciably within this 0.02 MeV interval, rotating the foil should have an appreciable effect on damage rate. From our measurements on polycrystalline platinum, we can determine that, for example, at 1.7 MeV the damage rate is changed by about 8% by changing the energy by 0.02 MeV, while at 1.5 MeV the same change in energy changes the damage rate by about 20%. These roughly estimated changes in damage rate caused by a degradation of energy of 0.02 MeV correspond quite well to the changes in damage rate from rotating the platinum foils (Fig. 6). Of course a more detailed analysis must account for the influence of nonuniform damage

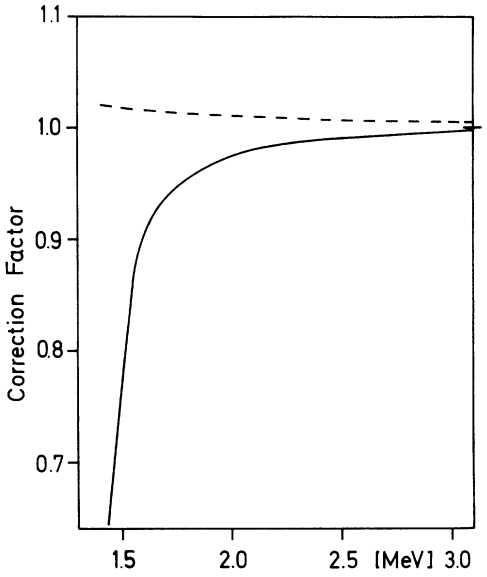

FIG. 6. The solid line shows the energy dependence of the experimentally determined correction factor, which must be applied to measured damage-rate values of 10-μm platinum foils when rotated to an irradiation direction 45° away from the normal direction. The dashed curve shows the effect which is expected from the increased multiple scattering of the electrons in the sample in a rotated position.

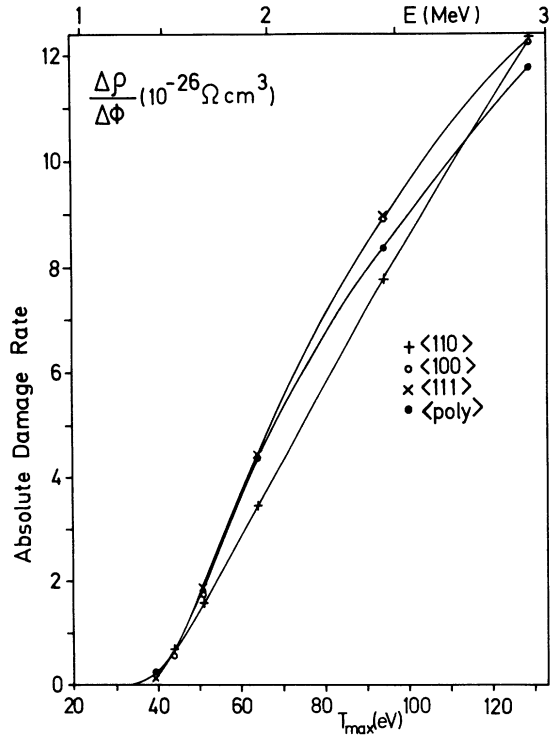

FIG. 5. Absolute damage rates of platinum single crystals and polycrystals versus maximum recoil energy T_{max}.

across the sample thickness on the measured damage rate at these low energies. For simplicity we used the experimentally determined correction factors shown by the solid curve in Fig. 6. In the case of copper this correction factor is at all energies lower than 1%.

IV. ANISOTROPY OF THRESHOLD ENERGY

The connection between the anisotropy of threshold energy $T_d(\Omega)$ and the dependence of damage rate $(\Delta\rho/\Delta\phi)(E, \Omega)$ on electron energy E and irradiation direction Ω in the crystal is given by the following equation:

$$\frac{\Delta\rho}{\Delta\phi}(E, \Omega) = \rho_F \int_{T(E,\Omega-\Omega')> T_d(\Omega')} \frac{d\sigma}{d\Omega}(E, \Omega - \Omega')\, d\Omega \,. \qquad (1)$$

In this formula the differential cross section $d\sigma/d\Omega(E, \Omega - \Omega')$ is integrated over all angles Ω' around the direction of incidence, where the energy $T(E, \Omega - \Omega')$, which is transferred from the electron of energy E to a lattice atom along direction Ω', exceeds the threshold energy T_d in this direction. In this integral the threshold energy acts as a limit of integration and defines that solid angle in which displacement is possible. To obtain the resistivity change of the samples per unit flux

of the irradiating electrons the integral must still be multiplied by ρ_F, the resistivity per unit concentration of Frenkel pairs.

As already mentioned, the electrons deviate from their initial direction of incidence by multiple scattering in the samples. There are two possibilities to include the influence of this effect in the above equation. One is to unfold the measured damage-rate data by the electron distribution. This method, explained in detail in,[4] is only applicable if damage rates are measured for a lot of directions covering the whole fundamental triangle. In the other case, an averaged cross section is used in Eq. (1) which is obtained by averaging the cross section of a monodirectional beam (Mott cross section) by the real angular distribution $dn/d\Omega$ of the electrons in the sample (compare Ref. 3):

$$\frac{d\sigma}{d\Omega}(E,\Omega)_{av} = \int_{T(E,\Omega') \geq T_d(\Omega)} \frac{d\sigma}{d\Omega'}(E,\Omega') \times \frac{dn}{d(\Omega-\Omega')}(E,d,\Omega-\Omega')\,d\Omega' \,. \quad (2)$$

This averaged cross section, $[(d\sigma/d\Omega)(E,\Omega)]^{-}_{av}$, not only depends on irradiation energy E and angle Ω between the direction of the electron beam and the knocked-on atom, but also on the threshold energy along the impact direction. That is, due to the fact that in the above integral the cross section of a monodirectional beam is cut off at an angle Ω', which corresponds to a transferred energy $T(E, \Omega')$ equal to the threshold energy T_d along Ω.

The electron distribution for multiple scattering, $dn/d\Omega$, is described by Molière's theory[14] and is given to a good approximation by the following equation:

$$\frac{dn}{d\Omega}(E,d,\alpha) = (\pi\bar{\alpha}^2)^{-1} e^{-(\alpha/\bar{\alpha})^2}, \quad (3)$$

where α is the angular distance between the electron beam and the angular element Ω. d is the thickness of the sample and $\bar{\alpha}$ gives the Gauss width of the distribution, which depends on the material and the thickness of the samples and on electron energy. It should be emphasized that Eq. (3) gives the electron distribution per solid angle Ω, while the distribution per angular distance $dn/d\alpha$ corresponding to this function is a Gaussian.

With the averaged cross section of Eq. (2) and an assumed threshold energy profile $T_d(\Omega)$, damage-rate values for different energies and irradiation directions were calculated by Eq. (1). In a trial-and-error fitting program, a good over-all agreement between these calculated damage rates and the measured values for the respective energies and directions was searched by systematically changing the threshold energy profile. For this, the whole fundamental triangle was subdivided in about 40 equal-sized regions with variable threshold values. A comparison was made to measured damage rates at five energies between 1 and 2 MeV in copper (Figs. 2 and 4), and at six energies between 1.5 and 3 MeV in platinum (Figs. 3 and 5), and for each energy, to eight irradiation directions along the border of the fundamental triangle. This means the fitting program used 40 damage-rate values in the case of copper and 48 in the case of platinum to determine the threshold energy profile.

In Fig. 7 two fundamental triangles for the cubic system are shown which are bounded by the three main symmetry axes and which contain all possible lattice directions. In the upper right-hand corner, the position of the fundamental triangle in the unit cell of a fcc lattice is shown. In these fundamental triangles, those regions, the threshold energy values of which fall in a certain range, are grouped together and the threshold energy range in every part of the triangle is given in eV by the inserted numbers. The discontinuities appearing sometimes between adjacent parts of the triangles are caused by the discreteness of the profile used in the computer fitting. As already mentioned these profiles were subdivided in areas of 5×5 degrees. More realistic profiles must have used a finer subdivision which, on the other hand, would have increased the errors of the threshold values in each individual area. The profiles given in Fig. 7 for platinum and copper are those that gave the best fit to our measured damage rates.

Owing to the rather complicated connection between damage rates and threshold energy in Eq. (1), it is difficult to give an exact error estimation for the values in Fig. 7. But the calculations showed that the lower the threshold energy is in a certain region of the fundamental triangle, and the more extended this region is, the more sensitive is the fit for variations of this value. On the other hand, in smaller regions or in regions of higher threshold energy the values may be changed to some degree without influencing the fit markedly.

The angular resolutions of the details in our profiles are of course limited by the number of measurements, the measuring accuracy, the influence of beam spreading, and the specific form of the cross section, which tend to mask finer details. On the other hand, fits as good as to the profiles in Fig. 7 are not possible to simpler profiles like, for example, the one proposed by v. Jan and Seeger[15] which expands the threshold energy along the first-order cubic harmonics using the threshold values along the three main crystallographic directions as free parameters. Naturally for a smaller number of measurements, such a simpler procedure is applicable, as was shown in the case of nickel by Bourret.[16]

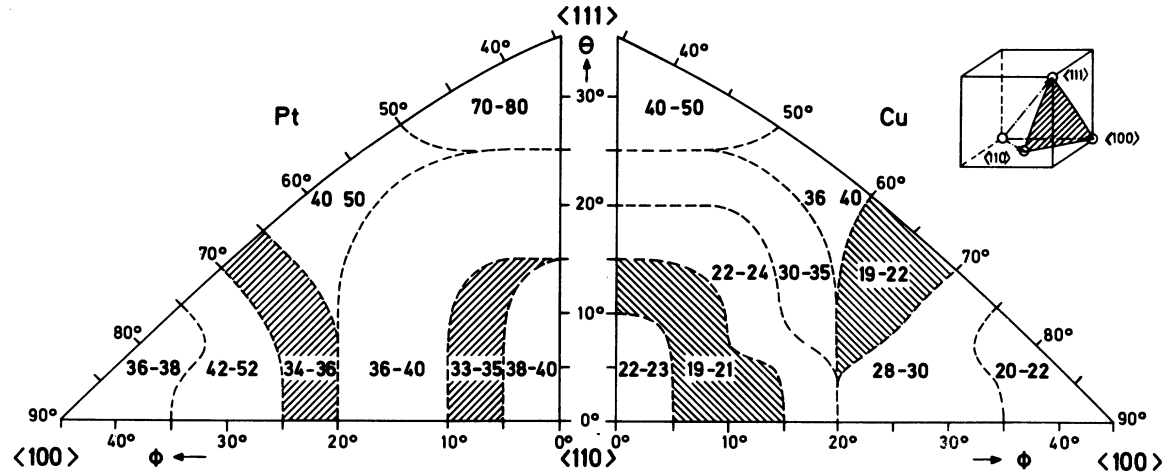

FIG. 7. Threshold energy profiles of plantinum and copper. The figures give the threshold energy range in every particular region. The regions of minimum threshold are shaded.

It is obvious from Fig. 7 that the resulting threshold energy profiles of copper and platinum are qualitatively rather similar. Of course the absolute threshold values of platinum are higher than those of copper, but in both metals the threshold energy is changing by about 100% within the profile. Further, the minimum threshold regions of about 33 eV in platinum and 19 eV in copper (shaded in Fig. 7) are lying around the two closest-packed lattice directions ⟨110⟩ and ⟨100⟩, while a pronounced maximum appears along the ⟨111⟩ direction. It is especially remarkable that the proper minimum is always attained somewhat off the ⟨110⟩ and ⟨100⟩ directions. In the case of the ⟨100⟩ direction also along the axis, threshold values are attained which are only 1 eV (that is within the error bars) higher than the values in the shaded regions. On the other hand, the minimum regions around ⟨110⟩ are only removed by 5° from the axis. Therefore the fact that minimum regions occur around the ⟨110⟩ and ⟨100⟩ directions is much more founded than the remoteness of the minima from these axes.

In Figs. 4 and 5 for copper and platinum an extrapolation of the damage-rate–vs–energy curves to the damage-rate zero for a determination of a minimum threshold energy (giving values of about 19 and 33 eV, respectively) seems straightforward, thanks to the steep onset of damage rate at these energies. But in copper samples finite damage rates far below a transferred energy of 19 eV have been found by Bauer and Sosin[17] and Iseler *et al.*[18] Till now, attempts to explain this effect have been made along two different ways. Bauer and Sosin[17,19] and Kamada *et al.*[6] ascribed this "subthreshold" damaging processes to so-called soft spots, e.g., light impurity atoms. The other explanation was given by Wollenberger and Wurm,[20] who suggested a small region with an angular radius of about 5°, e.g., around the close-packed ⟨110⟩ direction in copper, where they assumed a threshold energy falling down to values of about 10 eV. This last concept is favored by recent pinning experiments of Lücke *et al.*[21] who found threshold energies in copper, between 8 and 14 eV dependent on irradiation temperature.

A similar tail for the damage rate at low energies has been found in gold.[17] We looked for it in our high-purity polycrystalline platinum samples and found a displacement cross section of about 0.03 b for transferred energies below 33 eV, remaining nearly independent of energy down to 23 eV. This value is smaller than in copper by a factor of about 30. To explain this small cross section by a low threshold region with an threshold energy of less than 23 eV, this region must have an angular radius of less than 2 deg. Threshold energies which are bounded to such a small region give only a very small contribution to the cross section and therefore cannot markedly influence our fit. Therefore, as already mentioned, they cannot be determined with high enough precision.

In the fitting program for Eq. (1), the ρ_F values were determined giving an increase in resistivity per unit concentration of Frenkel pairs of $(9.5 \pm 0.5) \times 10^{-4}$ $\mu\Omega$ cm for platinum and about $(1.7 \pm 0.3) \times 10^{-4}$ $\mu\Omega$ cm for copper.

In the case of copper, the threshold energy profile of Fig. 7 was derived from our damage-rate measurements at energies between 1 and 2 MeV. But this profile also gives correct damage rates at energies below 1 MeV in agreement with Sosin's data.[5] On the other hand, we did not use in our calculations on copper the damage rates at energies

above 2 MeV, because for these higher energies the influence of multiple displacement may become appreciable. In multiple displacements one energetic impact from an electron to a lattice atom produces more than one Frenkel pair. The energy dependence of multiple displacements may be estimated, e.g., from the theory of Kinchin and Pease,[22] which predicts the onset of multiple displacements at about double the minimum threshold energy. As significant experimental results on this dependence are not yet available and as theoretical approaches[23] point toward an overestimation of the effect of multiple displacements by the Kinchin–Pease theory, we tested the influence of multiple displacement on our results by including a multiplication factor $\nu(T)$ in the differential cross section in Eq. (1):

$$\nu(T) = \frac{T(E,\Omega) - 2T_d(\Omega)}{2T_d(\Omega)} \quad \text{for } T(E,\Omega) > 2T_d(\Omega) \ . \tag{4}$$

This factor resembles the Kinchin–Pease prediction and therefore may overestimate the effect. With the inclusion of this factor, the resulting threshold energy profile showed a somewhat more pronounced anisotropy and a slightly lowered ρ_F value. Apart from this, the characteristic features of the threshold energy profile for copper shown in Fig. 7 remained unchanged.

Further assumptions, which are made in Eq. (1), are discussed in detail in Ref. 4. We only want to point to the assumption that the probability for producing a stable interstitial by an impact along lattice direction Ω jumps from 0 to 1 exactly at a recoil energy $T = T_d(\Omega)$ and stays unity for all higher energies. Some recent calculations of Torrens[24] not only show that the vacancy-interstitial separation is not steadily increasing with recoil energy, but also that at energies far above threshold, the attainable separation of the interstitial may decrease below the value reached at the threshold energy. As these results are very sensitive to the interatomic potential used in the calculations, some caution is recommended. On the other hand, as already shown for the case of multiple displacements, processes concerning high recoil energies do not influence our results appreciably as they have a comparitively small cross section.

V. DISCUSSION

It is interesting to compare our results on threshold energy with other investigations of this topic. This is only possible in the case of copper as platinum single crystals have not been used so far. There is first the work of Kamada *et al.*,[6] who used rather thick samples (100 μm) which were cut off the main crystallographic directions. These authors gave no details on the anisotropy of the threshold energy but reported only a minimum threshold-energy value of 28–30 eV, which is much higher than data of other authors.[5,17,18] Next there is the work of Sosin and Garr,[5] where for both the ⟨110⟩ and ⟨100⟩ directions, a threshold energy of about 19 eV was found in fair agreement with our results. These authors have already pointed out that it is impossible to obtain a threshold energy profile by only irradiating some crystals along the main crystallographic directions. This is due to the fact that damage is always possible within a cone around the irradiation direction. The opening of this cone is determined by the maximum transferred energy $T_{max}(E)$ and the threshold energy profile around the irradiation direction. Therefore, if at some angular distance Δ from the irradiation direction the threshold energy $T_d(\Delta)$ is lower than $T_{max}(E)\cos^2\Delta$, radiation damage will preferentially occur along this direction and not along the irradiation direction. Considering this, we can derive from our threshold profile of copper, where no lattice direction is separated from the minimum threshold regions (19 eV) by more than 20° to 25°, that the observable (effective) threshold for any lattice direction should be lower than (19 eV)/($\cos^2 25°$) ≈ 23 eV. Under these conditions it is interesting to consider the results of Makin,[25] who determined threshold energies by irradiating very thin copper single crystals in an electron microscope. In Table I the effective threshold energy along the three main crystallographic directions of copper are calculated from the distances Δ of these directions from the regions of minimum threshold (≈19 eV) in Fig. 7 and compared to the results of Makin. Both results are obviously in good accordance within the angular resolution of Fig. 7 (about 5°). This consideration may further show that this cosine-squared effect greatly reduces the advantage of thin samples, which avoid beam spreading by multiple scattering, as already explained in Ref. 26.

Furthermore, thin samples will possibly bring in effects like channeling, which in the case of very thin samples cannot be unambigously divided from the effects of an anisotropic threshold energy. This topic has already been discussed exten-

TABLE I. Comparison of effective threshold energies along the main crystallographic directions to the results of Ref. 25.

hkl	Δ[a] (deg)	$T_{d,eff} = \frac{19\ \text{eV}}{\cos^2\Delta}$	$T_{d,eff}$[b]
110	5–10	19.1–19.6	19.2
100	20–25	21.5–23.1	21.6
111	20–25	21.5–23.1	26.6

[a]Figure 7. [b]Reference 25.

sively in Refs. 26 and 4.

The high beam fluxes and the technique of observation in an electron microscope allow investigations only at elevated temperatures, where most defects are already mobile. This possibly makes a more detailed comparison of our low-temperature results and those from electron-microscope measurements difficult.

Next we will compare our results to the computer calculations for copper of the Brookhaven group.[1] In Fig. 8 the contours of our threshold energy profiles of Fig. 7, along the border of the fundamental triangle, are given and also the computer results[1] are included. For these calculations[1] a minimum threshold energy in copper of 25 eV was assumed by appropriately selecting the interatomic potential. This is higher than the more recent experimental values of about 19 eV. But apart from this, some remarkable analogies are visible between this profile, derived from a theoretical potential, and our profiles, derived from measured damage rates. In both cases the low-threshold-energy regions lie around the two closest-packed directions ⟨110⟩ and ⟨100⟩, and the high-energy region is situated around the ⟨111⟩ direction. Also, in both cases the absolute values of the minimum threshold energies around ⟨110⟩ and ⟨100⟩ are nearly the same. These results are qualitatively also in accordance with the data for bcc tantalum,[4] where large ring-shaped regions with low-threshold-energy values have been found around the two closest-packed lattice directions. On the other hand,

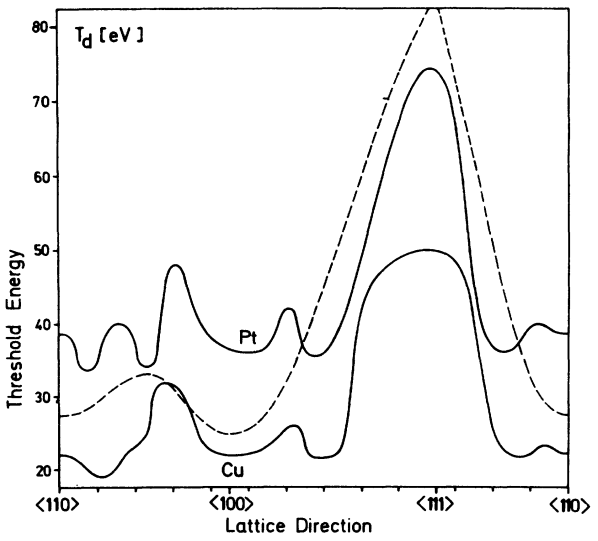

FIG. 8. Contour of threshold energy profiles from Fig. 7 of platinum and copper along the border of the fundamental triangle. The broken line corresponds to results of computer calculation of the Brookhaven group (Ref. 1).

TABLE II. Comparison of our threshold energies to those derived from Eq. (5).

hkl	$T_r(\Omega)$[a]	$d_{stab}(\Omega)$[a]	$\Delta T(\Omega)$[b]	$T_d(\Omega)$[c]	$T_d(\Omega)$[d]
110	17	4	≈1	21	22–23
100	11	2	≈5	21	20–22
111	50	1	≈30	80	40–50

[a]Reference 1. [c]Equation (5).
[b]Reference 28. [d]This work.

the computer results do not show as much structure as our profiles. This is mainly due to the fact that only very few calculations have been done outside the main crystallographic directions. To understand the details of our profiles, e.g., the fact that the minimum threshold is attained somewhat off the main directions, further computer simulations which may give more insight to defect production mechanisms would be desirable.

Finally, we will try to connect our results to other theoretical considerations on damage production. Starting from the impact an energetic particle transfers to a lattice atom along a certain lattice direction, there are two possibilities which may account for an anisotropic threshold energy: The first is that the separation between interstitial and vacancy, which is necessary to form a stable Frenkel pair, depends on lattice direction. An anisotropy of stability distance $d_{stab}(\Omega)$ in copper was already found by Gibson *et al.*,[1] and most of their results, for example, that separation must be largest along the ⟨110⟩ direction, are confirmed by a recent work of Scholz and Lehmann.[27] The second possibility is that it may be easier to obtain a separation of some atomic distances between the interstitial and its vacancy, along certain lattice directions. Some insight into this question was given by the investigations of Thompson and co-workers (e.g., Ref. 28), who found large differences in energy degradation $\Delta T(\Omega)$ for replacement-collision chains propagating along different lattice directions.

The connection between threshold energy $T_d(\Omega)$, stability distance $d_{stab}(\Omega)$, and energy degradation $\Delta T(\Omega)$ is given by the following equation:

$$T_d(\Omega) = T_r(\Omega) + d_{stab}(\Omega)\,\Delta T(\Omega)\,, \qquad (5)$$

where $T_r(\Omega)$ is the so-called replacement energy, which is necessary to start a defect-producing process along one of the main crystallographic directions. From Ref. 28 Eq. (5) may overestimate $T_d(\Omega)$ somewhat, because replacement sequences can indeed only be started at energies above T_r, but once started they may continue also at energies below T_r, favored by relaxation effects.

By Eq. (5) we can calculate now threshold energies $T_d(\Omega)$ using values for $T_r(\Omega)$ and $d_{stab}(\Omega)$ from

Ref. 1 and values for $\Delta T(\Omega)$ from Ref. 28. The resulting $T_d(\Omega)$ values are compared to our results in Table II.

The agreement is satisfactory and yet should not be overestimated as, e.g., Thompson *et al.*[28] obtained $T_r(\Omega)$ values which differ at least for the $\langle 110 \rangle$ direction markedly from those of Ref. 1.

ACKNOWLEDGMENTS

The authors are indebted to J. Viehweg for doing the epitaxial work. Thanks are also due to W. Kogler and his co-workers for operating the Van de Graaff. Further we gratefully acknowledge stimulating discussions with W. Schilling.

*Department of Physics and Astronomy, Clemson University Clemson, S. C. 29631.
[1]J. B. Gibson, A. N. Goland, M. Milgram, and G. H. Vineyard, Phys. Rev. **120**, 1229 (1960).
[2]C. Erginsoy, G. H. Vineyard, and A. Englert, Phys. Rev. **133**, 595 (1964).
[3]P. L. F. Hemment and P. R. C. Stevens, in *Radiation Effects in Semiconductors*, edited by F. L. Vook (Plenum, New York, 1968), p. 290.
[4]P. Jung and W. Schilling, Phys. Rev. B **5**, 2046 (1972).
[5]A. Sosin and K. Garr, Phys. Status Solidi **8**, 481 (1965).
[6]K. Kamada, Y. Kazumata, and S. Suda, Phys. Status Solidi **7**, 231 (1964).
[7]P. Wombacher, J. Phys. E **5**, 243 (1972).
[8]J. Wurm, F. Dworschak, H. Schuster, and H. Wollenberger, Rad. Effects **5**, 117 (1970).
[9]J. Wurm, Kernforschungsanlage Jülich, Rept. No. Jül-581-FN, 1969 (unpublished).
[10]W. Bauer and W. F. Göppinger, Phys. Rev. **154**, 584 (1967).
[11]E. A. Burke, C. M. Jimenez, and L. F. Lowe, Phys. Rev. **141**, 629 (1966).
[12]G. Duesing, W. Sassin, W. Schilling, and H. Hemmerich, Cryst. Lattice Defects **1**, 55 (1969).
[13]C. N. Yang, Phys. Rev. **84**, 599 (1951).
[14]G. Molière, Z. Naturforsch. A **3**, 78 (1948).
[15]R. v. Jan and A. Seeger, Phys. Status Solidi **3**, 465 (1963).
[16]A. Bourret, Phys. Status Solidi A **4**, 813 (1971).
[17]W. Bauer and A. Sosin, J. Appl. Phys. **35**, 703 (1964).
[18]G. W. Iseler, H. I. Dawson, A. S. Mehner, and J. W. Kauffman, Phys. Rev. **146**, 468 (1966).
[19]W. Bauer and A. Sosin, J. Appl. Phys. **37**, 1780 (1966).
[20]H. Wollenberger and J. Wurm, Phys. Status Solidi **9**, 601 (1965).
[21]K. Lücke, G. Roth, H. Wollenberger, and Ch. Zeckau (unpublished).
[22]G. H. Kinchin and R. S. Pease, Rep. Prog. Phys. **18**, 1 (1955).
[23]C. Erginsoy, G. H. Vineyard, and A. Shimizu, Phys. Rev. **139**, A118 (1965).
[24]I. M. Torrens (private communication).
[25]M. J. Makin, in *Proceedings of the International Conference on Atomic Collision Phenomena in Solids, Sussex, 1969* (North-Holland, Amsterdam, 1970), p. 205.
[26]W. Bauer and A. I. Anderman, Phys. Rev. **185**, 870 (1969).
[27]A. Scholz and Ch. Lehmann, Phys. Rev. B **6**, 813 (1972).
[28]M. W. Thompson, in *Defects and Radiation Damage in Metals* (Cambridge U. P., London, 1969), p. 222.

PHYSICAL REVIEW B VOLUME 8, NUMBER 2 15 JULY 1973

Magnetoacoustic Wave in an Electron-Hole Gas—Bismuth. II. Effect of Anisotropy and Landau Damping in a Geometry where $\vec{q}$ is not Perpendicular to $\vec{B}$

C. Guthmann, J. P. D'Haenens, and A. Libchaber
Groupe de Physique des Solides, Ecole Normale Supérieure, 24 rue Lhomond, Paris V, France*
(Received 16 October 1972)

We present here a general study of the propagation of magnetoacoustic waves in bismuth for arbitrary directions of the propagation and of the magnetic field, at a frequency of 3 GHz. Compared to the geometry $\vec{q} \perp \vec{B}$ described in a previous paper, new experimental facts appear. The coupling of the acoustic mode to the Alfven wave can be observed for magnetic field values much higher than those observed in the geometry $\vec{q} \perp \vec{B}$. This change in coupling is related to a strong increase of the electron-hole-gas kinetic pressure. Also, Landau damping of the acoustic mode is observed. A full analysis of these phenomena is given here, experimentally and theoretically, and we present also a magnetohydrodynamical model of these effects.

I. INTRODUCTION

In a previous paper,[1] hereafter referred to as I, we gave a theoretical and experimental description of magnetoacoustical modes, sustained by an electron-hole gas for a propagation direction perpendicular to the magnetic field. With the spectrometer in the 3-GHz frequency range described in I, we are able to study propagation for every angle of the wave vector $\vec{q}$ with the magnetic field $\vec{B}$. New experimental facts appear: (i) a strong increase of the electron-hole-gas effective kinetic pressure, which results in a coupling of the acoustic mode to the Alfven wave at a magnetic field much higher than that observed in the geometry $\vec{q} \perp \vec{B}$; (ii) Landau damping of the acoustic mode.